Analysis of Straw Tracker Properties and Gas Blendings

Julia Larsson Dahlberg, Adam Jonsson, Elin Ring, Andreas Ström, Jonathan Törnquist and Elias Waagaard

Under the Direction of Hans Danielsson and Richard Skogeby

CERN, Geneva, 2016

Abstract

The NA62 straw detector, utilized in experiments of the underground LHC particle accelerator at the European Organization for Nuclear Research (CERN) and whose headquarters are located on the border between France and Switzerland, provides an excellent tool to detect cosmic particles such as muons in the quest for completing the gaps in the Standard Model, a step towards a better understanding of the universe. A straw detector, i.e. a cathodic tube containing a Penning mixture of noble gases and quench gases, with an anodic straw in the middle enable a voltage difference to be maintained. By investigating the signal amplitude from the ionization and its electron avalanches of charged incoming particles, information of the properties of these cosmic particles can be extracted. We investigated phenomena such as the cosmic radiation background, gas gain and signal wave propagation. Upon assumptions from these experiments, we developed models for the cosmic radiation background, gas gain, ionization frequency over distance and time dilation of the signal. These models could to a large extent be confirmed by technical supervisors and third-party sources, although sources of error raised question marks in some of our conclusions.

Table of Contents

Introduction

As extremely energy-dense cosmic particles reach the upper atmosphere, the energy bursts make new short-lived arise, which thunder down towards the surface of the Earth and decay into new particle showers. A prime example of this phenomenon is the muon ($\square^-$), which forms at an altitude of dozens of kilometers[1]. As the muon knocks out electrons at such relativistic energies, an avalanche of electrons is unleashed and can be picked up by detector electrodes, for instance the Resistive Plate Chamber at the CMS experiment at CERN[2]. However, on rare occasions exotic particles are being formed and reveal their presence by decaying into secondary particles. One of the NA62 experiment objectives is to study the rare decay $K^+ \rightarrow \square^+ V\bar{\nu}$. According to the Standard Model of physics (SM) the semileptonic branching ratio (BR) for this decay is

$$BR(K^+ \rightarrow \square^+ V\bar{\nu})(SM) = (8.5\pm0.7)\square 10^{-11}$$

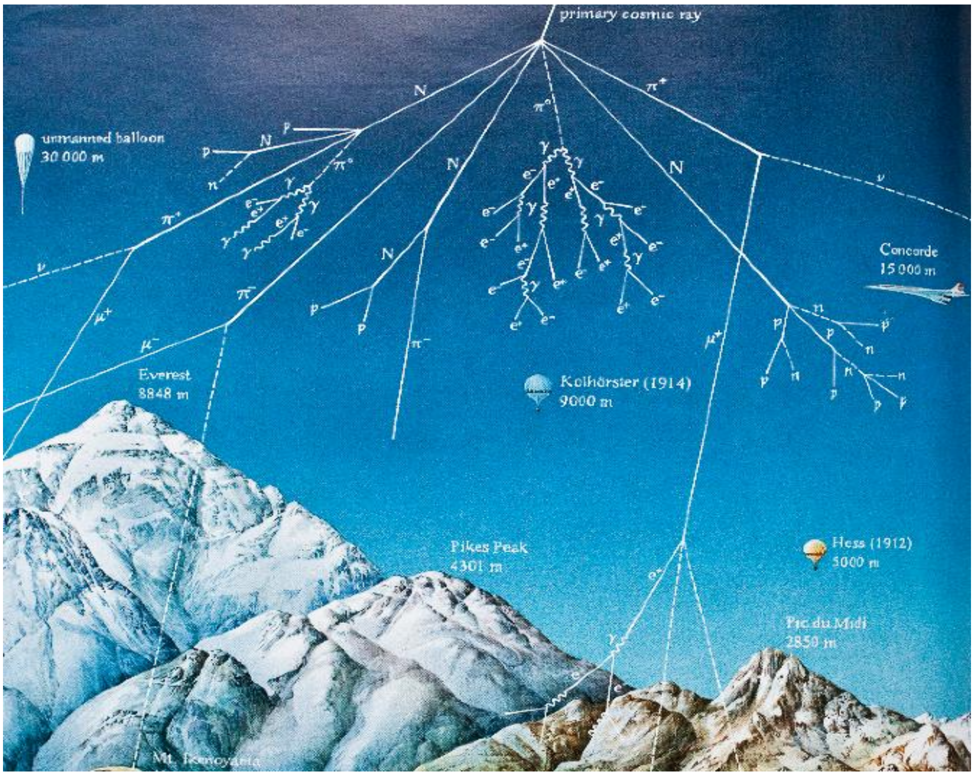

Figure (1), Decay of Particles From Cosmic Rays, Source: www.cargocollective.com

The uncertainty of the theoretical BR is dominated by the current precision of the CKM mixing matrix parameters rather than by theoretical errors affecting the hadronic matrix

[1] Boezio, M., Carlson, 2000
[2] CMS Tracker Detector, CERN, 2011

element. Thanks to the E787 and E949 experiments at Brookhaven National Laboratory by studying kaon decay, the BR consistent with the Standard Model have been estimated[3] to

$$\mathrm{BR}(K^+ \rightarrow \pi^+ V\bar{\nu}) = (1.47 \, {}^{+1.30}_{-0.89}) \times 10^{-10}$$

The large discrepancy in errors between the theoretical and the experimental motivates the NA62 experiment[4], which is designed to measure decays of this type with an experimental uncertainty rate better than 10%.[5] To better distinguish the charged kaon decay track, which supposedly belongs to the pion, from the overwhelming background cosmic radiation, the main kinematic variable of the squared missing mass was used

$$m^2_{miss} = (p_{K+} - p_{\pi+}).$$

Ultimately, this is one additional step to confirm the predictions of the Standard Model or to resort to alternative models. We believe that this straw tracker prototype will achieve the objectives of the various technical aspects, such as the detection of cosmic radiation and reliably track the ionization caused by a radiation source, listed below.

Questions for experimental set-up

The experiments are originated from following statements, which will be answered in the report.

1) Estimate the frequency of cosmic radiation passing per square second.
2) Determine an expression for the gas gain as a function of the high voltage using simulated data for a gas mixture of 70 %/30 % Ar/CO_2 and 85 %/15 % Ar/CO_2, and use it to properly compare the signal amplitudes and efficiency, with respect to the high voltage, of the two gases.
3) Develop a model for the detected frequency of ionization with respect to distance of the radioactive source
4) Develop a model for the propagation of the signal depending on where the primary ionization takes place

[3] Artamonov, A. V., Bassalleck
[4] NA62 Official Website
[5] Martellotti, Silvia

Background

Straw Tracker

Straw tracker is a type of gaseous ionization detector that measures direction and momentum of secondary particles. When cosmic radiation decay in the atmosphere a small amount reaches the surface and interacts with a tube filled with a gas mixture consisting of argon and carbon dioxide. The tubes consists of 36 μm thick PolyEthylene Terephthalate (PET) film metallised with 50 nm of copper, to keep the gas at a stable concoction, to not exposure any air to the gas, and 20 nm gold, to get the minimum resistance to the current, to minimizing the heat output. Each straw has a 30 μm gold-plated tungsten wire in the center.

The gas mixture is under high voltage creating an anode and a cathode. The anode is in the middle of the tube, along the wire and the cathode is along the tube's edge. Electrons (e^-) attracts to the anode and due to a strong electronic acceleration by the electric field

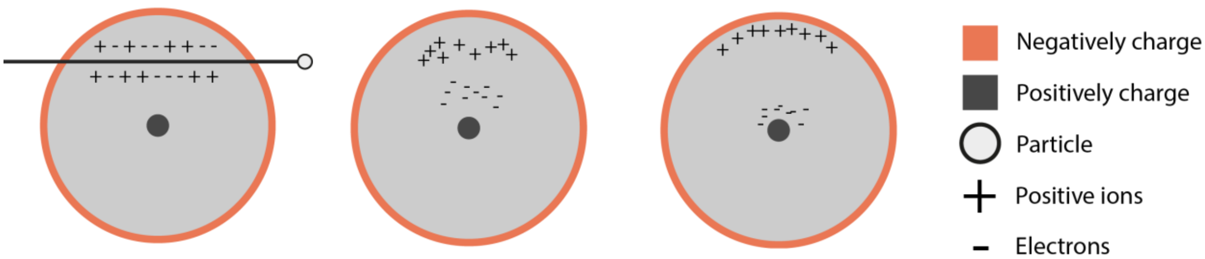

an avalanche starts[6].

Figure (2): Schematic cross-section of straw tracker and gas ionization through interaction of incoming high-energy particles.

This avalanche is a chain reaction and happens when free electrons collide. There is two possible outcomes for the avalanche, as illustrated below in Figure (3):

1. Input electrons around the gas molecule absorbs kinetic energy from an accelerating electron and excites an electron (e^-). Excited electrons from the ground state will after a short period of time fall back into the ground state and send out photons. The output electron loses kinetic energy and movement.

2. Electron ionization and a higher kinetic energy of electrons leading to further atom collides and electrical conductive plasma that is measured in the straw tracker.

[6] Straw Tracker Technical Description

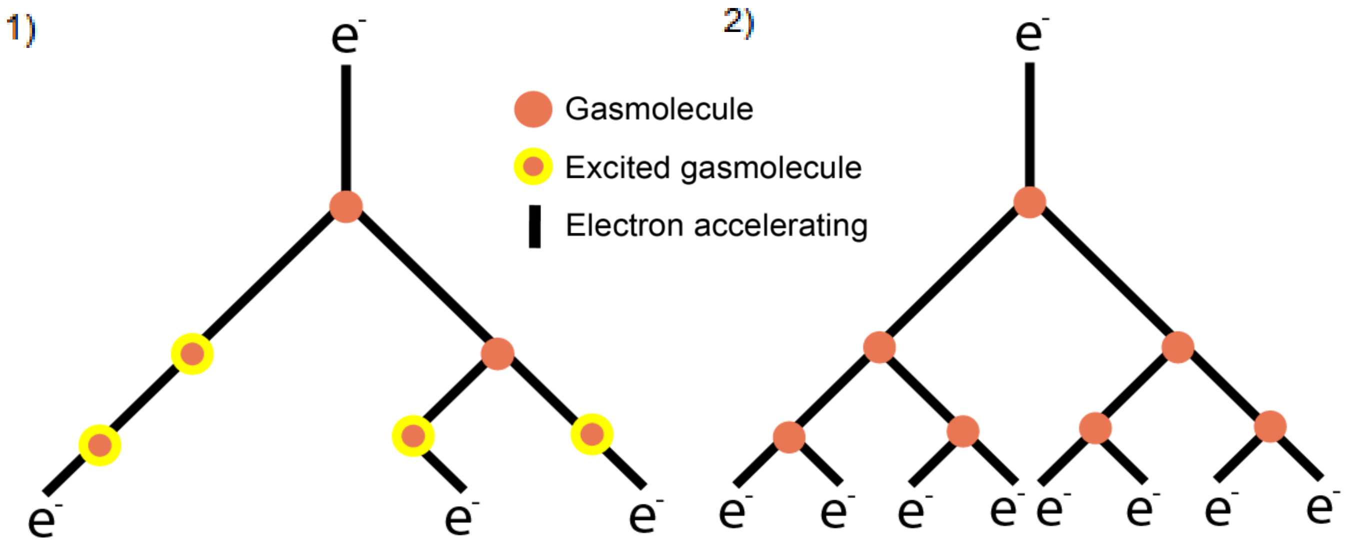

Figure (3), Illustration of avalanches caused by high-energy electrons.

As of today, many of the experiments carried out at CERN rely on straw detectors to obtain high-quality measurements[7]. There are many advantages with this technique in comparison to conventional drift tubes:

- Simple low-cost construction
- The detector chamber is built in modules, which facilitates complicated detector geometry
- High resolution can be achieved with more straw chambers
- A malfunctioning or broken wire in the tubes is isolated from its neighbors.
- Neighboring straws are electrically shielded which minimize corrupting crosstalk.
- Straws can operate at high-rate environments with relatively good spatial resolution.
- Straws can be made self-supporting and eliminates the need of a framework structure.

One of the main disadvantages with the straw detector tubes is the amount of material added to the detector, which marginally augments the particle interaction and radiation length of the chamber[8]. Another major disadvantage is the multiple scattering occurring in straw detectors, i.e. the variance of particle positions and directions change multiple times. As a result, the tracing of mother particles, such as kaons and pions, is impeded. The more the material introduced in the detector chamber, the more variance there is and the more multiple scattering occurs.

[7] NA62 Read-out System Description, 2010
[8] Marzec, J., Zaremba, K, 2000

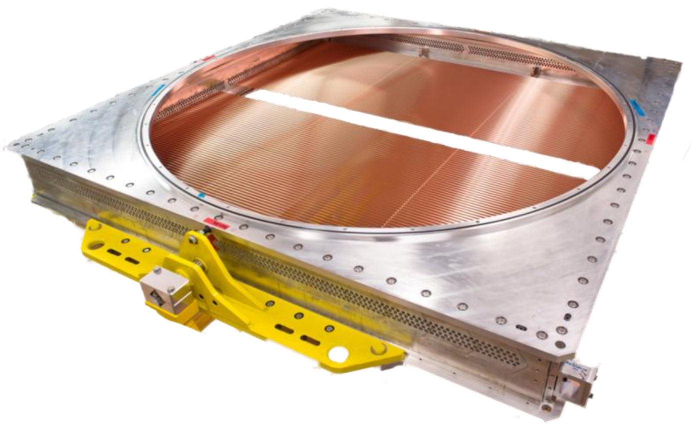

Figure (4), Close-up View of Straw Module with Horizontal and Vertical Tubes for 2D Coordinate Registration of Incoming Particle. Source: <https://ep-news.web.cern.ch/sites/ep-news.web.cern.ch>

However, microelectronics have in recent years greatly improved the accuracy and functionality of the straw trackers, since Charpak's fundamental idea of this detector. Charpak, who worked at CERN, won the Nobel Prize in physics 1992 for his invention of the multiwire proportional chamber and for increasing the data collection speed, by connecting the detector directly to a computer. His inventions have been of decisive importance for many discoveries in particle physics during the last two decades.[9]

Method and Measurements

The oscilloscope trigger level was set to the same value for all measurements (-250 mV), in order to avoid voltage noise. The number of sweeps on the oscilloscope was adjusted for every analysis, depending on how much signal frequency registred. It was set to 100 sweeps while measuring the frequency of cosmic radiation and was increased up to 100 000 sweeps when measuring the signal amplitude of gas mixtures for the gas gain. When the frequency was measured with respect to distance of the radioactive source and when measuring the propagation of the signal depending on where the primary ionization took place, the number of sweeps was 2000. For every analysis when the radioactive source was involved, the number of sweeps could be set up higher, since more particles leads through the tubes, compared with measuring the frequency of cosmic radiation when only background radiation goes through the tubes, which noticeably goes slower. Because of time constraints, the number of sweeps was low when the radiation source was not used.

[9] Nobelprize.org

Experimental Set-up

The purpose of the experiments is to analyze the technical functions of a straw tracker by investigating the ionization of particles affected by cosmic radiation and a radioactive source. The execution of the experiments were limited to one week, which did impede a follow-up of more precise measurements.

The oscilloscope that was used is a Wave Runner 104MXi-A with a frequency up to 1 Ghz and 10GS/s. With this instrument, we calculated voltage, mean, standard deviation and time; including a minimum trigger level to reduce detecting noise. The trigger level was set to -250 mV as a threshold in order to avoid voltage noise and thereby get measurements of the important cosmic radiation signals. The number of sweep represents the average of that specific parameter, where one sweep constitutes one measurement. Also used was a prototype of NA62 straw module, a radioactive source (^{55}Fe), a gas mixture of 70%/30% Ar/CO_2, a gas mixture of 85%/15% Ar/CO_2 and a voltage central.

#1: Cosmic Radiation Frequency

High-energy photons, protons as well as larger atomic nuclei are at a high rate smashing into Earth's atmosphere. From the impact with the molecules in the atmosphere and due to the large energies involved, secondary particles are created. These then split into tertiary particles and so on. A tiny fraction of the particles originating from these collisions reach all the way down to Earth.

One the objectives were to determine the frequency (Hz) of these "cosmics" passing through us per square meter (m^2). We decided to measure the frequency (Hz), the deviation voltage (ΔmV) and the standard deviation (SD) depending on the high voltage using the straw detector and the oscilloscope. Another thing needed to get accurate readouts was for us to not regard the background radiation or the smaller deviations in the tech. This was avoided using the 'trigger' function on the oscilloscope, we estimated that we needed this to have a value of -250 mV to not pick up the deviations we were not looking for. This was possible because the cosmics have a higher energy than the other things mentioned.

The actual problem in this task was that the frequency of signals changed depending on the level of high voltage run through the detector when it was a known fact that we couldn't change the frequency of the cosmics. However, when we in retrospect looked at our plot we realised that the frequency stabilized at about 1850 V for a value of around 10 Hz.

We then proceeded to assume that this was because of the avalanches of multiple electrons (e^-). The reason for this being that the e^- needs to reach a critical velocity to start an avalanche. As a result of this it cannot do that before reaching the anode because of its lower velocity in a weaker electrical field. After the electrical field reaches that critical voltage (which for this mixture of gas was 1850 V) it does not matter how much stronger the field gets because the avalanches are still being produced above that point. With this said, Paschen's law is another factor limiting the strength of an electric field. The length of straw was estimated to be 2.355 m, whereas its diameter (0.098 m) was given on forehand. The frequency *f* for the cosmic radiation was estimated to

$$2.355m \cdot 0.0098m = 0.023079m^2$$

$$f = 10Hz$$

$$\frac{f}{0.023079} = 433.2943368Hz/m^2.$$

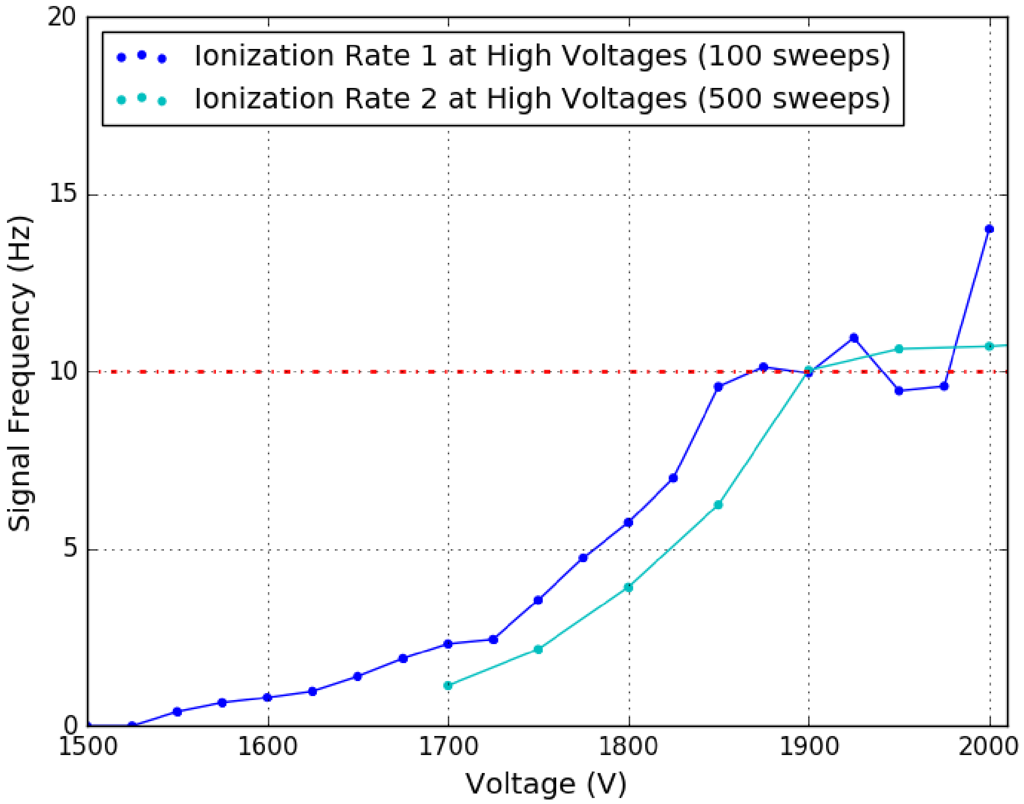

Figure (5), Ionization Rate as a Function of High Voltage Due to Cosmic Particles, where the dashed red line shows at what voltage the straw detector reaches maximum efficiency and gives the most accurate value of signal frequency.

According to Paschen's law, there is a minimum voltage, the so-called breakdown voltage, necessary to cause an electric discharge between two electrodes as a function of gas pressure and gap length. In our straw detector, both the the gap between the anode wire and cathode double-foil and the gas pressure of the tube remain constant. Consequently, as the high voltages of the detector is successively augmented, the breakdown voltage threshold will be reached and electrical arcs (discharges) will cause an increase in ionization before the electrical circuit shuts down. This explains the ultimate peak after the frequency functions plateaus. In addition, Paschen's law also put forth that this breakdown voltage is somewhat proportional to the mass of the gaseous medium. Therefore, a detector tube filled with mostly argon will have a lower breakdown voltage, in contrast to a gas mix with a heavier gas (CO_2 in this case) that will have a higher breakdown voltage before any electrical discharges. This explains why the voltage interval for ionization is shifted towards lower values for the enriched argon mixture with only 15 % CO_2, whereas the 70 % Ar/ 30 % CO_2 mixture will have higher lower and upper bounds for the voltage.[10]

#2: Gas Gain and High Voltage

Gas gain is the magnitude by which the signal is increased from the primary ionization to the collection of charge at the anode. That is, a secondary particle interacts with the gas particles in the straw and ionises the particles, thus creating free electrons. These are then attracted by the positively charged anode and therefore starts accelerating inwards, towards the anode. The acceleration gives the electrons enough energy to knock out other electrons from the gas atoms and ionise them, which creates an avalanche of electrons. When the electrons have reached the anode the ionization stops, and the quotient between the primary ionization and the number of ionization created which makes up the gas gain. Normally, noble gases exhibit high inertia since there are few ways in which an atom can lose energy apart from excitation and ionization[11]. In order to prevent multiple pulsing of electrons, which would contaminate the final results, a quench gas of 5-10 % of organic vapour or halogen gas with lower ionization voltage are used, together constituting a so-called Penning mixture.[12] In these experiments, a higher ratio of quench gas (in this case CO_2) in proportion to the noble gas was used to enable operation at higher voltages.

In this study, two gas mixtures with different $Ar\text{-}CO^2$ ratios were investigated in terms of gas gain as a function of high voltages. Out data points, an exponential fit model was then extracted for each of the cases, as seen in Figure (6). The exponential function corresponding to the gas gain G_1 as a function of voltage V for the 70% Argon and 30 % CO_2 was estimated to be

$$G_1 = 0.0360563064 \cdot e^{0.00591908361V}.$$

The exponential function corresponding to the gas gain G_2 as a function of voltage for the 85% Argon and 15 % CO_2 was estimated to be

---

[10] Wadhwa, C.L. (2007). *High Voltage Engineering* (2nd ed.). New Age International. pp. 10–12. ISBN 8122418597

[11] Chakravarty, S., & Armitage, J. C. (1992)

[12] Glenn F Knoll. 2000, ISBN 0-471-07338-5

$$G_2 = 0.0383785909 \cdot e^{0.00650490515V}.$$

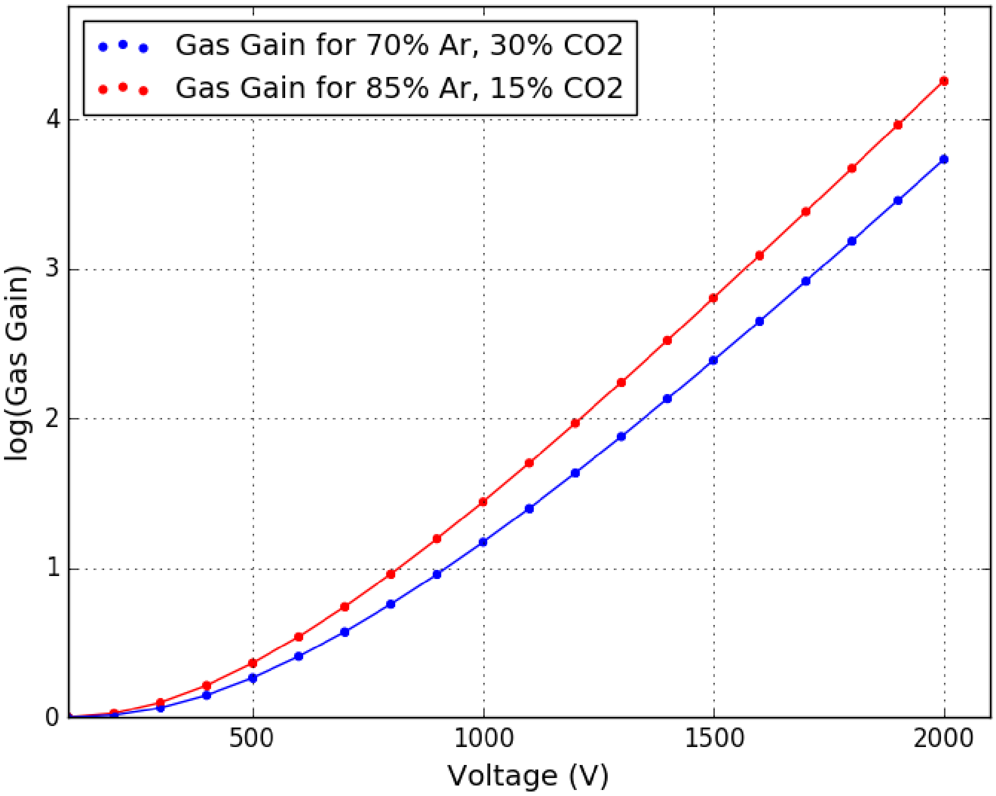

Figure (6), the Gas Gain as a Function log scale which clearly shows that the two functions are both exponential starting at roughly 750 V, the threshold values for the straw detector to operate with the respective gas mixtures.

Before any models could be created, we had to consider the fact that the different gas blendings had a respective lower voltage threshold before any frequent signals could be registered and optimize at 100 %. These exponential models were fitted to the scatter plots when the values for the voltages below the critical value were removed (>1500 V and >1300 V respectively) in order to reach a detectable frequency of ionization.

Due to the fact that the resistance increases in the straw tubes as the temperature increases, since electrical energy transforms to thermal energy, means that the functions of gas gain will heighten even more at higher voltage, which results in exponential functions as seen in the diagrams above. In the beginning of the functions it is as good as linear and that is because of the low thermal resistance since the voltage is low.[13]

[13] Pålsgård, Kvist, Nilson (2011) Ergo fysik 1, pp. 270-272

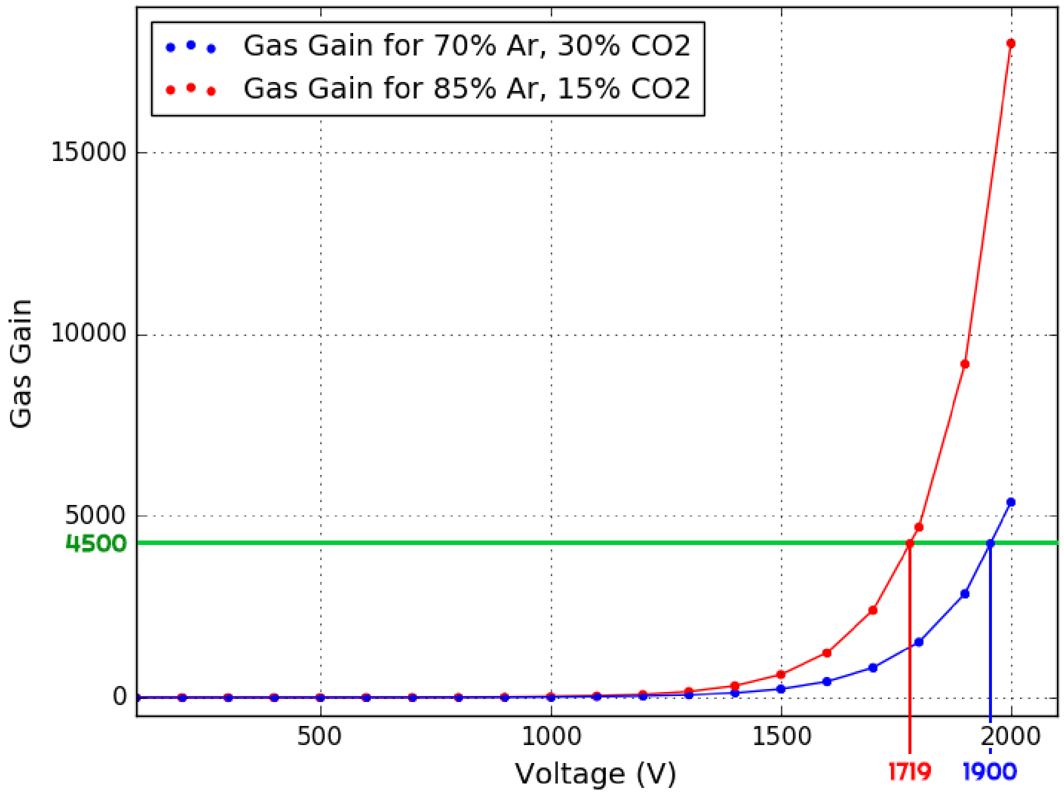

Figure (7), showing that same value of gas gains gives two different voltages for the respective gas mixtures that were investigated.

With these models as a benchmark, the respective signal amplitude of the voltages for the same gas gain value were then investigated. The two mixtures were investigated with a set gas gain value of 4500, giving two respective voltages as seen in Figure (7). By using this model, the voltage of the 85% Ar/ 15% CO_2 gas mixture was set to 1719 V whereas the voltage for the 70% Ar/ 30% CO_2 mixture was set to 1900 V as seen in Table (1).

Table (1), The average signal amplitude and its standard deviation as a function of voltages set a priori of a similar gas gain value. Two surveys of 10 000 sweeps and one survey of 100 000 sweeps were carried out for the respective gas mixtures and voltages. The trigger level was set to -250mV in order to reduce background noise.

% of gases in mixture	Voltage (V)	Average Signal Amplitude (-mV)	Average Standard Deviation (mV)
70 Ar/ 30 CO_2	1900	2584.7	663
85 Ar/ 15 CO_2	1719	2913.6	387

We detected a difference between the signal amplitude in the respective gas mixtures, with a prominently higher value for the 85% Ar/ 15 % CO_2 mixture. In these sweeps, a much lower standard deviation was obtained also for this blending, implying a much lower spread around the average signal amplitude. This might be an indication that the 85% Ar/ 15 % CO_2 has a chance to provide more uniform and therefore reliable results to investigate different properties of secondary decay particles at different voltages. However, the elevated value of standard deviation undermines such a conclusion, especially for the 70/30 mixture, as the difference is smaller than the standard deviations, thus signalling the need for further measurements.

#3: Ionization Frequency with Respect to Distance

^{55}Fe has a half life of 2.737 years and it decays into ^{55}Mn. This was the source used to determine the different ionization frequencies depending on the distance between the radioactive source and the detector. This aspect provides important insights in the sensitivity of the straw detector for the type of radioactive decay mentioned above. As the radiation intensity is inversely proportional to the distance from the source, a reliable model had to be considered for the straw tracker using the ^{55}Fe sample. Obviously, fewer ionizing particles, e.g. electrons or alpha particles, reach the straw detector if they traverse a large distance with a higher probability to encounter and ionize molecules in the surrounding air. Since radiation scatters in all direction, we resort to the equation for the area of a circle

$$A_{sphere} = 4\pi r^2.$$

With this principle of the spherical area and presuming that the source is static, we can derive the intensity function as a function of distance in centimeters

$$I(d) = \frac{x}{4\pi d^2} + R$$

where *I* is the radiation intensity in Hertz registered by the detector, *d* is the distance in centimeters between the straw tracker and the radioactive sample, *R* is the background radiation originating from cosmic rays and that was estimated to 10 Hz in Figure (8), *x* is a constant to adjust for the distance unit, since our distance measurements were carried out in centimeters. In Figure (8) however, the constant *R* was set to 11Hz for a better fit. When *x* was set to 7000, a good fit starting distance *d* was obtained.

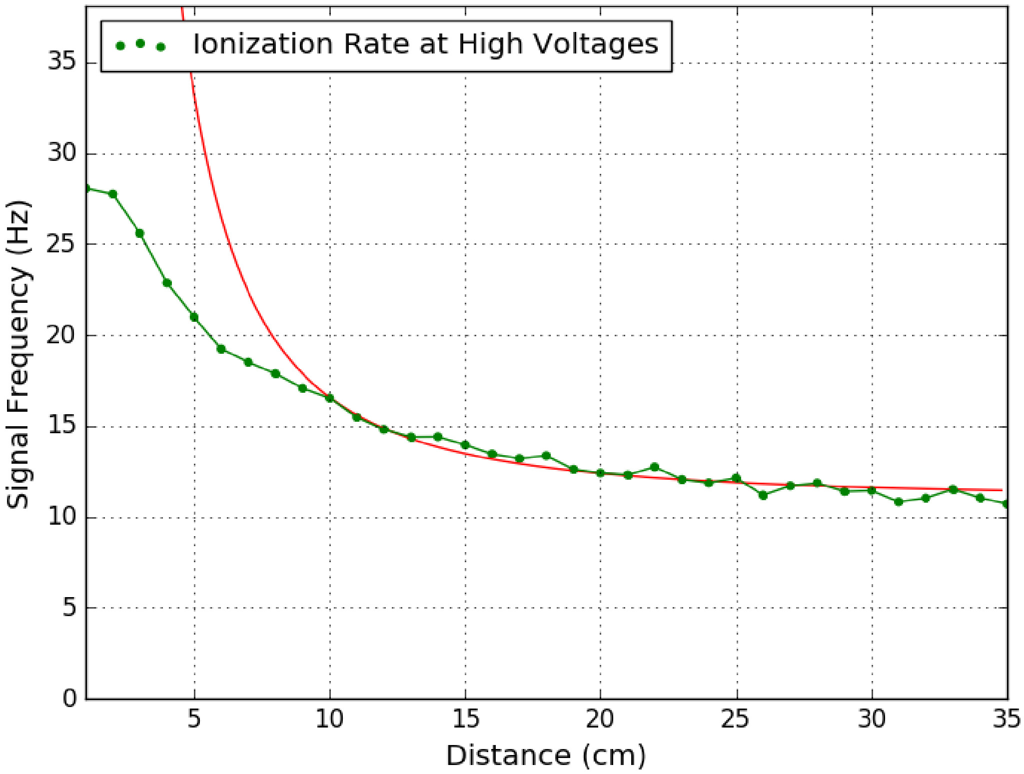

Figure (8), Ionization rate as a function of the distance to the radioactive source, where the frequency decreases as the distance to the radioactive source increases.

Since practical obstacles such as the outer foil of the straw tube impede measurements conducted at distances lower than a few centimeters, the rational functions is not valid for a small interval. Unlike the rational function $I(t)$ which reaches infinity as d reaches 0, the actual level of radiation crosses the signal frequency values at $I = 30$. This model described above satisfy the need for accuracy for $d = 10$ and onwards, although another function for the interval $0 < d < 10$ would therefore be needed.

#4: Propagation of the Signal

The task was to figure out a way to determine the propagation of the signal after the primary ionization (PI) in the straw, depending on how far from the front-end electronics (FEE) it happened. The straw detector signal represents a deviation in the electrical field, which occurs when the electrons and/or ions moved closer to the anode respectively cathode. The signal itself can therefore be described by a wave motion in the electrical field.

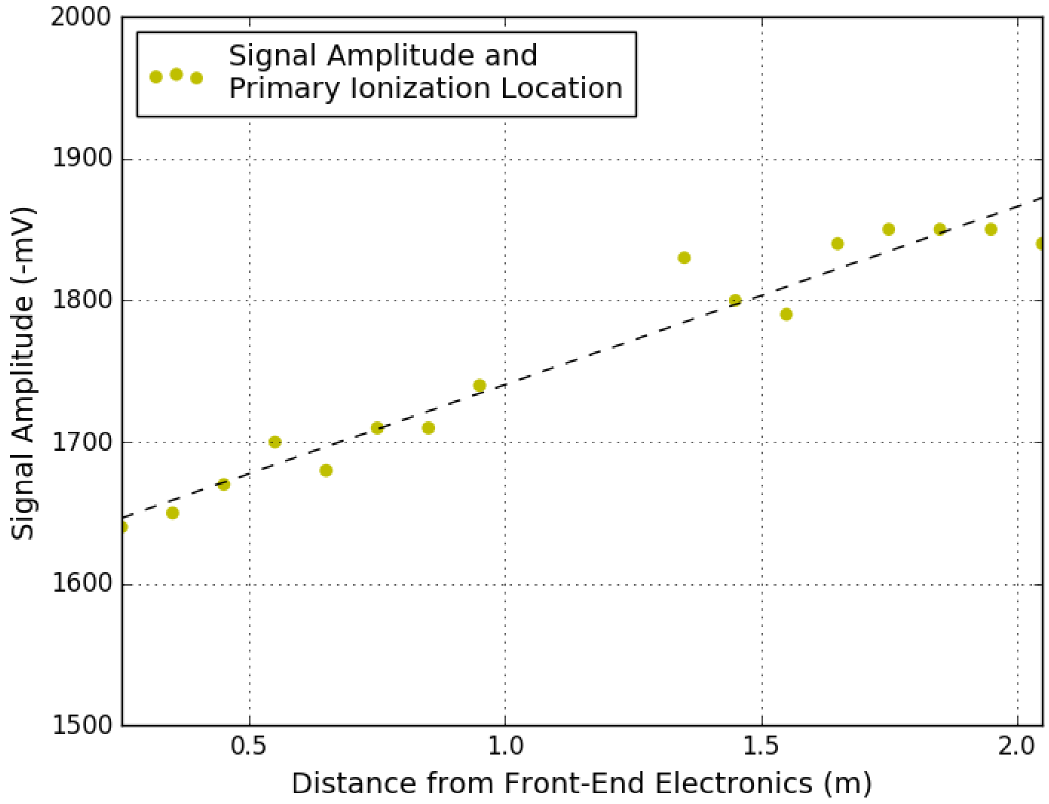

Figure (9), Signal Amplitude as a Function of Distance to Front-End Electronics (FEE), where the linear trend is marked with a dashed line.

Through the utilization of a radioactive ^{55}Fe source and measuring the difference in signal amplitude (ΔmV) depending on the distance between the PI and the FEE, we found that the signal amplitude was higher the further away the source was from the FEE, as seen in Figure (9). Other parameters, such as frequency as a function of distance from the PI to the FEE, were also investigated. However, that presumption was discarded since there was no significant difference. The results in Figure (9) indicates a proportional relationship between the signal amplitude and the distance.

As seen below, when a pulse, or signal wave, traverses into a new medium, depending on the two different mediums properties, part of the pulse continues and the other part reflects back. However, in the experiment, the “more dense” medium had a resistance of close to ∞. This rendered the transmitted pulse too small and thus negligible, a cause for why almost the entire pulse was reflected back to the FEE, a possible reason for the linear trend in Figure (9).

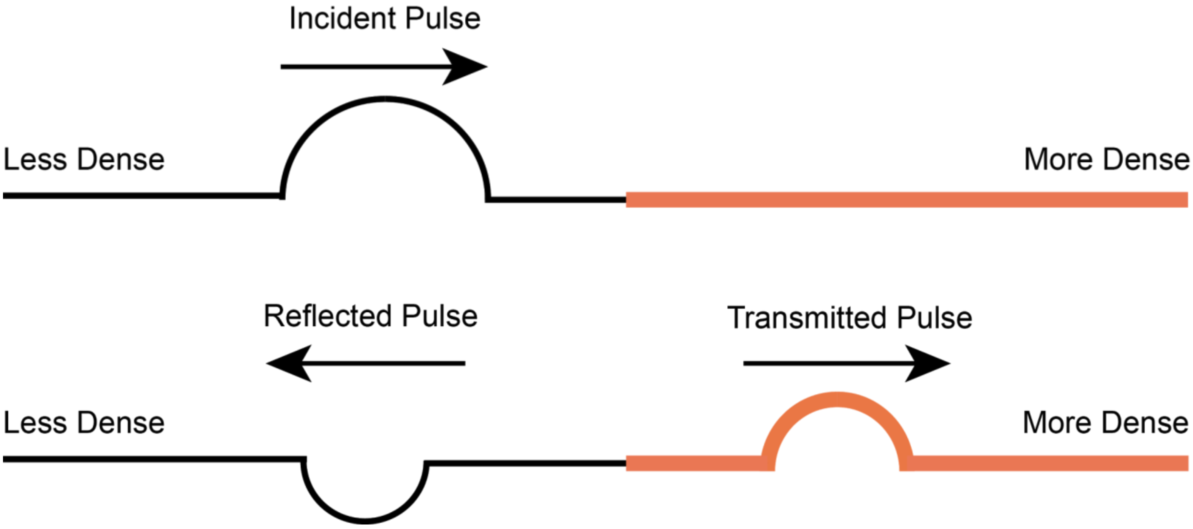

Figure (10), the general concept of a wave before and after traversing the edge between two different mediums.

Another factor that had to be counted in was the way in which the extremities of a straw tube are constructed, the wave motion that propagates through the tungsten wire is reflected similarly to a 'loose end' where the signal bounced without inverting its signal, as seen Figure (11) below. There are different ways to achieve different 'bounces' although our experiment comprised an open end and an identical signal reflection whereas an a closed end would have provided results similar to Serie A in Figure (11) with an inverted signal reflection.

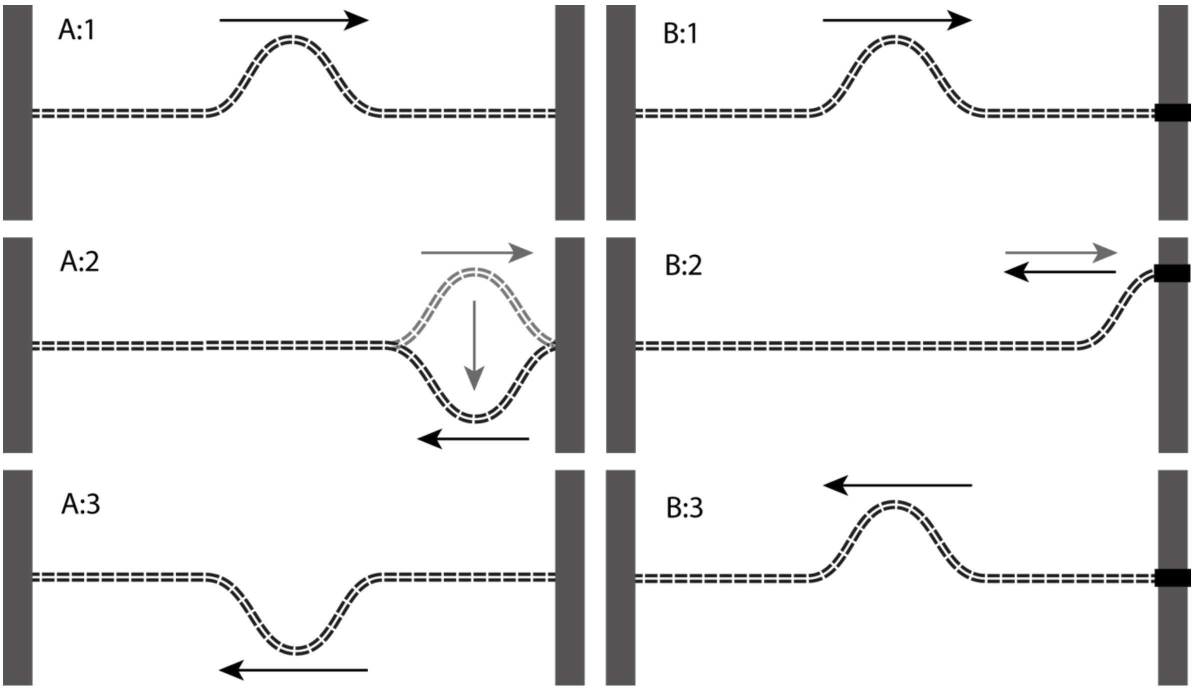

Figure (11), Explanation of Wave Reflection with Different Endings: Closed End (A) and Loose End (B).

With closed end (series A) to the back end instead of the loose end (figures B), the signal waves would have experienced destructive interference instead of the constructive one, as was demonstrated in this experiment. Since the waves were indeed undergoing constructive interference, the oscilloscope read out these waves as one unit, due the principle of superposition. The oscilloscope could only measure whole tens of ns (10^{-8} s) and the waves themself move so close to the speed of light that the difference was negligible. The signal (voltage difference) propagates close to the speed of light, whose travelling time back and forth in the straw tube is known because the length is also known

$$s = tc \qquad t = \frac{2 \cdot 2.355}{c} \approx 16ns.$$

If the waves move a maximum distance of the length of the straw times two, at the speed of light. That leaves us with a time of travel of about 16 ns which means that the oscilloscope picks up both the waves at what it believes is the same time and the sweep shows us one signal which is more or less amplified by what the oscilloscope registers to be a superposition.

However, there is another possible scenario that could be implemented in the straw detector of having an infinite loop for the signal. In the current straw detector version, the signal is reflected by adding inerting thickness to the wire as seen in Figure (10). An attenuation of the signal occurs in the straw, since the straw has resistance. Once there is a attenuation of the signal in the straw, this concept needs to be taken into account while determining the propagation of the signal. Since the attenuation weakens the signal, one would get a linear function where the strongest signal would be closest to the FEE, with a completely absent reflection of the signal. A visual representation of this infinite ending (which would thin the signal out until fading completely), instead of reflecting it back to the FEE, as is illustrated in Figure (12) below.

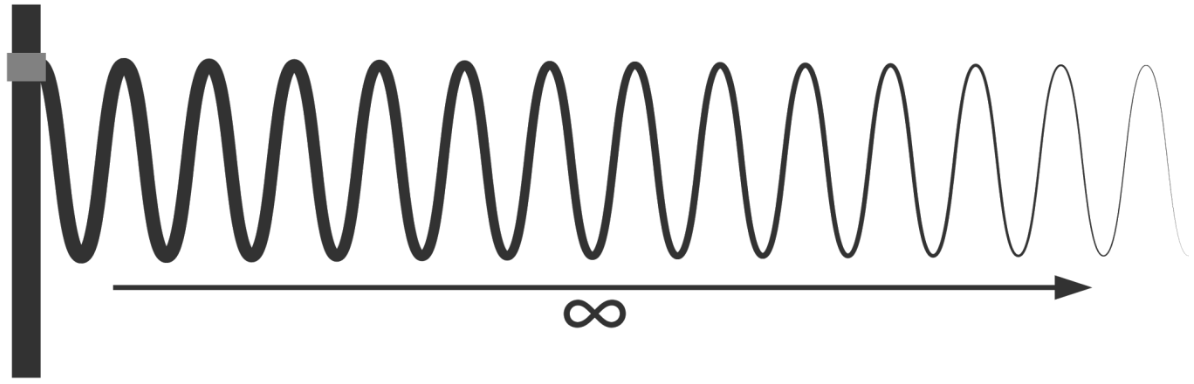

Figure (12), visual representation of an infinite loop.

Time Dilation of Signal Wave

How the signal propagates along the wire in the straw tube depends on the location of the primary ionization. As previously mentioned, a superposition of the signal wave plays a crucial role in the detection by the FEE. Two signals waves travel in opposite directions from the primary ionization, illustrated by the yellow dot in Figure (13), where a radiation source of ^{55}Fe is positioned.

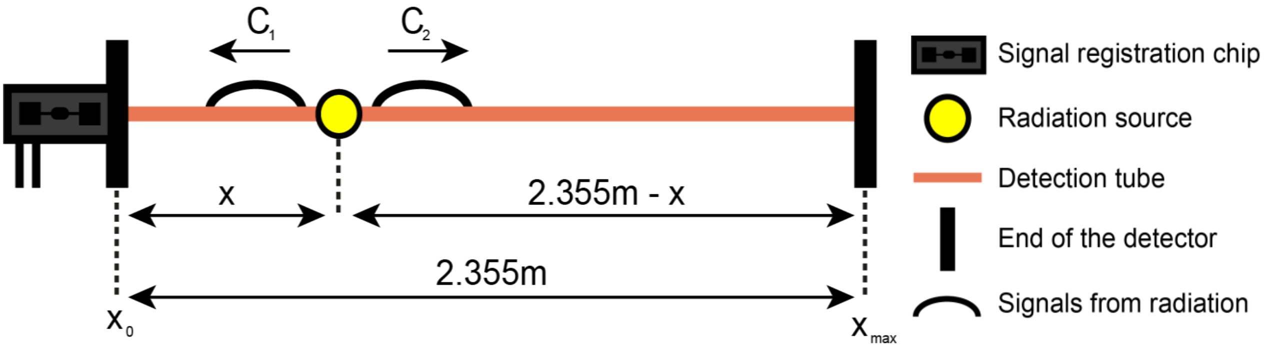

Figure (13), Cross-section diagram of straw detector signal propagation.

Consequently, the signal waves are denoted as C_1 and C_2 in Figure (13) . The distance C_1 travels is equal is denoted *x* whereas the distance C_2 travels is equal to $2(2.355 - x) + x$. However, if the variable *y* then represents the length of an arbitrary straw detector the second distance is rewritten as $2(y - x)+x$, where *y* in our experiments is set to 2.355 meters. A system of equations can then be formulated, based on the equation $s = vt$, where the signal wave velocity *v* is close to the speed of light *c*

$$x = c \cdot t_1$$
$$2(2.355 - x) + x = c \cdot t_2$$

and t_1 and t_2 denote the times required for the signal to travel for the waves C_1 and C_2 respectively

$$t_1 = \frac{x}{c}$$
$$t_2 = \frac{2(2.355-x)+x}{c}$$

give that the difference in time Δt is extracted from

$$\Delta t = t_2 - t_1$$
$$\Delta t = \frac{2(2.355-x)}{c}.$$

Followingly, as the length of the straw detector covered by the signal wave is very small in comparison to the propagation speed, the time delay Δt turn out to be tiny. In Figure (14), the theoretical time dilation, predicted by our model, is plotted as a function of distance to the FEE for the primary ionization.

To further illustrate the composition of time delay in the straw detector system, the propagation of the signal waves waves C_1 and C_2 is shown in Figure (15) below. The direction is denoted with a small arrow, and the registered signal is denoted with flashing green light on the FEE diodes.

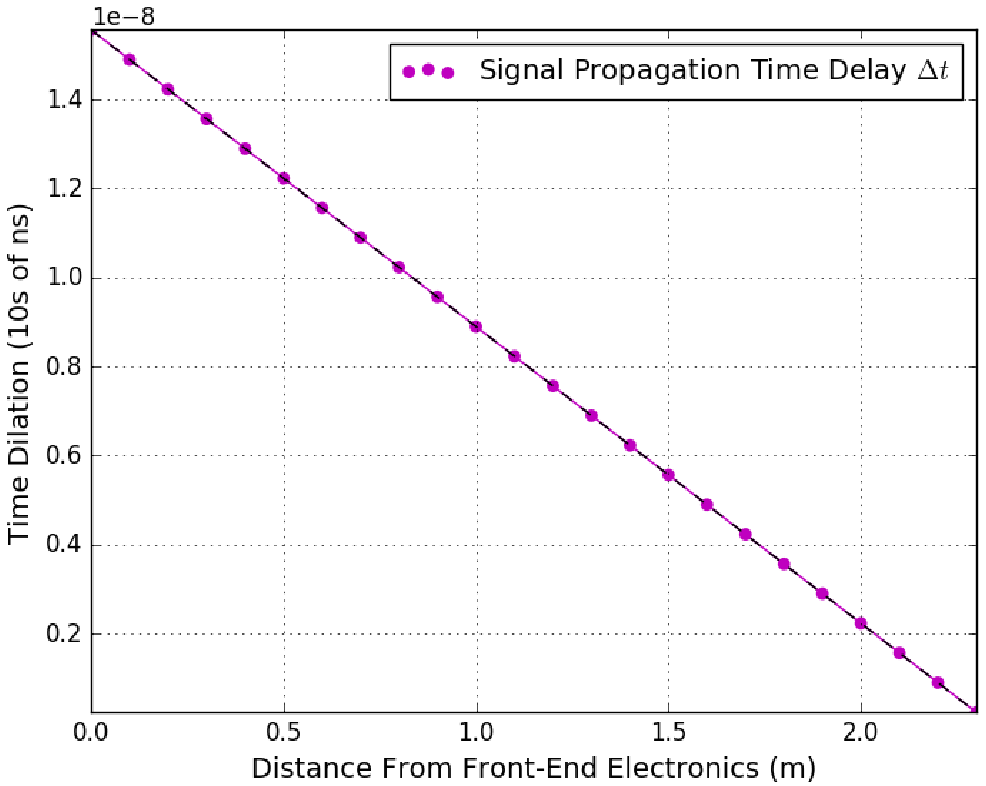

Figure (14), Time dilation between the signals as a function of distance from the front-end electronics FEE, where the time dilation is reduced as the distance increases.

In situation A:1 in the series, the radiation source provokes ionization in the tube gas mixture. This results in an almost immediate propagation to the chip for signal wave C_1 after the ionization. On the other hand, the signal wave C_2 propagates towards the other end of the detector. As C_2 reaches the end, it is reflected back towards the FEE as seen in situation A:2 and A:3. Finally, the C_2 signal is registered by the FEE (A:4).

In a scenario where the primary ionization is located much further away from the FEE, a smaller time delay Δt is obtained (B:1 to B:4). By calculating the time dilation between incoming signals leads enables us to estimate where the ionisation has taken place and thus where the cosmic ray has hit the straw detector, also for an arbitrary straw detector length y.

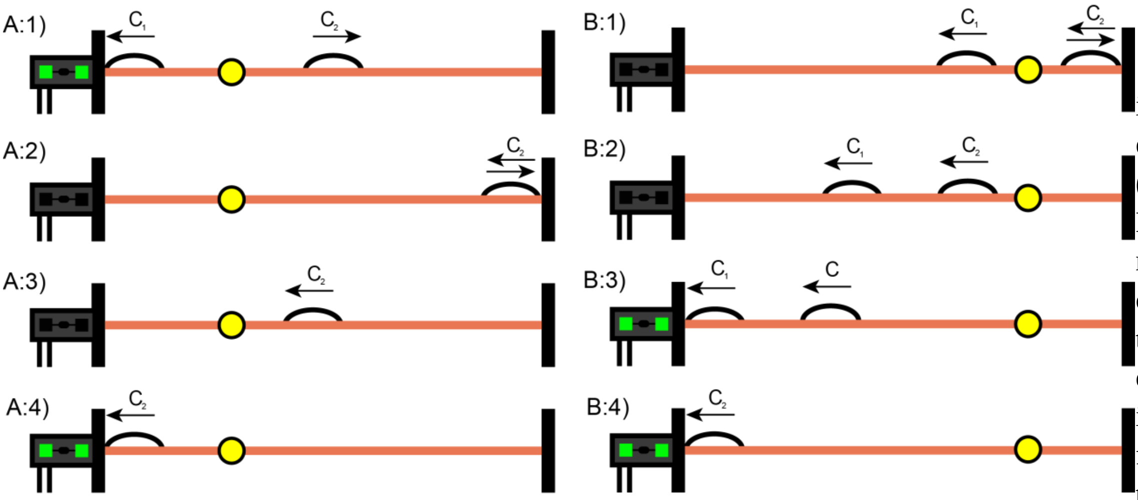

Figure (15), Diagram of time dilation for two signal waves in the straw detector as a result of ionization.

Accordingly, a model for calculating the distance to the primary ionization *x* in relation to the time delay *Δt* is set up

$$x = 2.355 - \frac{c\Delta t}{2}.$$

Signal Amplitude in Respect to Chip Distance

A time delay *Δt* will lead to a difference in amplitude in respect to chip distance. If we place the radioactive source closer to the front-end electronics (FEE) the time delay will be bigger, resulting in a smaller amplitude due to less interference between C_1 and C_2. The further away radioactive source from FEE is positioned, the higher the amplitude. This is a result of an interaction between the signal waves C_1 and C_2, leading to a wave superposition and an amplitude augmentation as seen in Figure (16).

Figure (16), Illustration of an exaggerated signal wave superposition

The dotted line in Figure (16) represents the actual amplitude A_1 and A_2. As the primary ionization is closer to the far end, a bigger interference occurs because of a smaller time dilation, resulting difference in signal amplitude in respect to distance from the FEE. A larger distance from the FEE would therefore mean a higher signal amplitude: a larger registred signal.

Consequently, there are locations in the straw tube where the primary ionization are distorted the most by maximum of the signal-wave interference. This could possibly be in the very center of the tube, or slightly closer to the opposite side of the FEE. With this principle of superposition as a result of the signal-wave reflection in mind, a possible explanation for the higher signal amplitude at higher distances from the FEE in Figure (9) emerges with our theory predicted in Figure (14) and the equations that follow.

Discussion

The final outcome of our experiments was successful, as the whole set of questions was answered. Even though our measurements of the cosmic radiation levels in the atmosphere somewhat coincided with the commonly accepted levels[14] but with small variations. This made even our supervisors question their previous results, demonstrating the needs of experiments constantly testing new and old theories. Our models of gas gain levels might even facilitate future construction of such experimental devices with higher accuracy and predictability of the behaviour of straw detectors. As demonstrated in Figure (8), the dogmatic spherical model of radiation propagation only applied to after a distance of 10 cm for the source. Is this a sign that the source itself did not behave linearly to a certain point of closeness, or that the top performance of the straw detector had already been reached and no more radiation could be registered? Regarding the ionization frequency with respect to distance to radiation source, a flaw in the model is that it is only valid after a certain distance. A possible explanation for why the observations do not match the expected values for signal frequencies for values lower than d = 10 cm is that the radioactive source in itself has a limited maximum for the radiation intensity.

Nonetheless, some sources of error could have affected our models and assumptions. The oscilloscope had system errors like vibrations and electronic noise, which we tried to avoid by setting a trigger level as a threshold, in order to measure the signals. One factor of uncertainty was to adjust the trigger lever right. If the trigger level was too low, the electronic noise would be registred as signals. In that case, the measurements contain evidently a degree of incorrectness. We would have to do more measurements to get more trustworthy results. We could also have missed possible factors that affects variables and this might have lead to wrong measurements, such as other local radiation or electronic sources. There is always a physical variation of cosmic ray and particle decay, where cosmic ray will always be randomized. This leads to uncertainty in our measurements over a certain time span, for instance if radiation levels are different during the day than during the night. With systematic measurements over a long period of time, this factor could have been eliminated. However, due the time limitation of one week for the internship, we reduced the number of sweeps and repeats for this experiment. More sweeps would have given us more accurate and reliable results. The time delay between incoming signals was in the straw

[14] M. Boezio, 2000

detector around tens of nanoseconds (~10^{-8} s) and precision limit of our oscilloscope was very close to that, resulting in a relatively high level of uncertainty. Despite these sources of error, a clear correlation between time dilation and signal amplitude was deduced by comparing the registered signal amplitude as a function of distance from the FEE in Figure (9), and our prediction of time dilation as a function of distance from FEE in Figure (14). To further confirm this model extracted from our experiments, even more precise equipment would be needed for these small time margins, for instance an oscilloscope capable of measuring nanoseconds or fractions of nanoseconds (10^{-9} to 10^{-10} s).

The human source of error could have affected the results, since we counted the mean and standard deviation from eye to paper. There is always a probability that we wrote a number wrong or miscounted an equation, since the device was constantly updating and might have changed by few decimal points or more from true value to interpretation. Also, our use of instruments and tools could affect the results. Other factors of uncertainty are, for instance, that the straw tube did not detect all particle decay or the gas mixture ratio was not 85 % argon/15 % carbon dioxide. This error could have been overcome by a series of standardization of instrument operations prior to the real experiments, which we unfortunately did not have time for.

However, the validity of our models still persists despite these sources of errors, being a good incentive for future studies.

Conclusion

To conclude, the purpose of this experiment was achieved by analyzing the functions of the straw tracker and investigating the ionization of cosmic radiation and the radioactive source. Through experiments, we succeeded to answer all problem statements with different levels of certainty.

The frequency of cosmic radiation passing per square meter per second was estimated to 433.3 Hz/m^2, stabilizing at 1850 V for a value around 10 Hz, as seen in Figure (5). We also concluded that the breakdown voltage, the maximum voltage for the ionization model, had to be taken into account according to Paschen’s law, which would explain the different properties exhibited by the two gas blendings.

We concluded that the ideal models to describe the gas gain, the magnitude by which the signal is increased from the primary ionization to the collection of charge at the anode, was set to $G_1 = 0.0361e^{0.0059V}$ for gas mixture 1 (70% argon/ 30% CO_2) and to $G_2 = 0.0384e^{0.0065V}$ for gas mixture 2 (85% argon/ 15% CO). The significant figures were adjusted to a lower level since the source of errors for the standard of error was relatively elevated.

The model we developed for the detected the frequency of ionization with respect to distance of the radioactive source (Fe^{55}), was that the frequency decreases as the distance to the radioactive source increases, proportionately to the area of a sphere, as seen in Figure (8). We concluded that the model only applied after a distance of 10 cm, probably due to an imperfect radiation propagation.

When developing a model for the propagation of the signal depending on where the primary ionization takes place, we concluded that the time dilation decreases as the distance to the end of the detector decreases, as seen in Figure (14). The time dilation between first and second signal wave is: $\Delta t = (2(2.355-x)/c)$. We empirically succeeded to confirm that a lower time dilation between two signal waves increased the signal amplitude in a linear trend, as seen in Figure (9).

Acknowledgements

We ardently thank NA62 coordinator Dr. Hans Danielsson and the CERN organization for making this fantastic internship possible. We also thank our lab instructor and mentor Mr. Richard Skogeby (CERN) for great guidance in this field, for vital advice and for evoking tremendous interest by showing us the various CERN experiments. In addition, we also thank the SMART project, Bromangymnasiet and EU for funding and for providing this opportunity to us. Throughout this lab course, we have met amazing particle physics scholars from all over the world and gained life-changing insights in the constituents of the universe.

References

1. Boezio, M., Carlson, P., Francke, T., Weber, N., Suffert, M., Hof, M., ... & Cafagna, F. “Measurement

2. Taylor, L. “Tracker Detector | CMS Experiment.” Tracker Detector | CMS Experiment. November 23, 2011, <http://cms.web.cern.ch/news/tracker-detector>, retrieved October 28, 2016

3. Artamonov, A. V., Bassalleck, B., Bhuyan, B., Blackmore, E. W., Bryman, D. A., Chen, S., ... & Frank, J. S. (2008). New measurement of the $K^+ \rightarrow \pi^+ \nu \nu$ branching ratio. Physical review letters, 101(19), 191802.

4. “CERN Accelerating Science.” NA62, <https://home.cern/about/experiments/na62>, retrieved October 28, 2016

5. Martellotti, Silvia. "The NA62 Experiment at CERN." arXiv preprint arXiv:1510.00172 (2015). <https://arxiv.org/pdf/1510.00172v3.pdf>, retrieved on November 17th 2016.

6. “1.1 Straw Tracker - Na62.web.cern.ch.”, <https://na62.web.cern.ch/NA62/Documents/Chapter_StrawTracker_extract_full_doc_v10t.pdf.>, retrieved October 28, 2016

7. “The NA62 Straw Detector Read-out System.” December 27, 2010, <https://cds.cern.ch/record/1321585/files/JINST5.C12053.pdf>, retrieved October 28, 2016.

8. Marzec, J., Zaremba, K., Pawlowski, Z., & Konarzewski, B. “Signal propagation in straw tubes with resistive cathode.” IEEE Transactions on Nuclear Science, <http://ieeexplore.ieee.org/stamp/stamp.jsp?tp=&arnumber=826893&tag=1>, retrieved October 28, 2016

9. “Press Release.” Press Release: The 1992 Nobel Prize in Physics, <https://www.nobelprize.org/nobel_prizes/physics/laureates/1992/press.html>, retrieved October 28, 2016

10. High Voltage Engineering, 2nd edition. New Age International. Pp. 10-12, Wadhwa, C.L 2007, ISBN: 8122418597

11. Chakravarty, S., & Armitage, J. C. (1992). A study of the gas gain in carbon dioxide mixtures. Nuclear Instruments and Methods in Physics Research Section A:

Accelerators, Spectrometers, Detectors and Associated Equipment,321(1), 186-194. Available at <http://ac.els-cdn.com/016890029290387J/1-s2.0-016890029290387J-main.pdf?_tid=c064fb2e-9fa6-11e6-9475-00000aab0f01&acdnat=1477945102_bbebc472cebe5e8f0135835f70c87dcf>, retrieved on October 31, 2016

12. Glenn F Knoll. *Radiation Detection and Measurement*, third edition 2000. John Wiley and sons, ISBN 0-471-07338-5 <http://journals.aps.org/prl/pdf/10.1103/PhysRevLett.101.191802>, retrieved on November 17th 2016

13. Jan Pålsgård, Göran Kvist and Klas Nilson. Ergo fysik 1: ISBN:9789147085538

14. M. Boezio et al., “On the flux of atmospheric muons with the CAPRICE94 apparatus.” Physical Review D. July 12, 2000, <http://journals.aps.org/prd/abstract/10.1103/PhysRevD.62.032007>, retrieved October 27, 2016